Analytical modeling of space-based thermal imaging systems

James A. Dawson
Dynetics, Inc.
Jason M. Gallaspy
Dynetics, Inc.
Charles T. Bankston
Dynetics, Inc.
David Scott Stanfield
Dynetics, Inc.

Abstract

Thermal imaging systems based on infrared focal-plane arrays provide a means for passive surveillance of space objects without the requirement for direct solar illumination. While such systems are readily available, their performance levels are usually described in terms of terrestrial objects and backgrounds rather than those associated with the space environment. However, given proper consideration of the specifics of the detector technologies used by the system, valid estimates for performance in the space object surveillance role can be readily obtained through analytical modeling. This paper reports the development of an approach for such analytical modeling. This approach is applicable to problems such as the design of space-based thermal imaging for viewing low-altitude space debris. The approach addresses key parameters for staring IR focal-plane arrays such as dark current as it relates to the current induced by background flux. Another critical consideration is the radiant intensity of the object to be viewed by the imaging system. Accurate knowledge of the radiant intensity is required in order to derive an optimal design for a space-based thermal imager. To support the modeling and design requirements, an empirical method for estimating the radiant intensity is needed. The use of an empirical method prior to commitment to a space-based design can overcome the uncertainty of modeling the thermal properties of space objects such as debris with unknown composition. To address this, the analytical modeling approach is extended to include ground-located thermal imaging systems such as would be used for measuring the radiant intensity of space objects. To illustrate the modeling approach, design examples are posed based on reported thermal imaging technologies. The sensor parameters include optical transmittance and temperature, noise-equivalent temperature difference (NETD), and dark current.

1. Introduction

The use of optical technologies for surveillance of space objects has relied mostly on visible systems due primarily to advantages in cost, simplicity, and sensitivity. In recent years this trend has been reinforced with improvements in resolution for both CCD and CMOS devices used as part of visible imaging systems. In addition to the availability of advanced technologies, in many instances the use of visible systems is driven by the requirement to resolve the target with sufficient detail to support recognition, identification, and characterization. Regardless, unless an active source is used to illuminate the target, the full level of performance requires solar illumination of the target. In the case of space objects at relatively low altitudes, this can be a severe handicap due to the significant

likelihood of shadowing effects of the earth and since this leads to many cases for which the space object will lack solar illumination.

To illustrate the concerns due to low-altitude objects in earth shadow, Fig. 1 depicts the geometry of interest. The figure shows a simplified case in which an object follows a non-inclined circular orbit about the earth. The object is assumed to be relatively small with an apparent area of 400 cm^2. The portion of the orbit for which the object will be in shadow can be easily computed using trigonometry. This leads to the probability that the object is in earth shadow as given by Eq. 1, where h is the altitude of the object and R_e is the radius of the earth.

$$P_{shadow} = \frac{\theta}{2\pi} = \frac{1}{\pi}\sin^{-1}\frac{R_e}{R_e + h} \tag{1}$$

Using this equation, such space objects with altitudes below 1000 m will be in shadow between 33% and 40% of the time. This is a significant problem and motivates consideration of thermal imagers that should essentially work 100% of the time albeit with potential reduction in maximum range and increased cost and complexity.

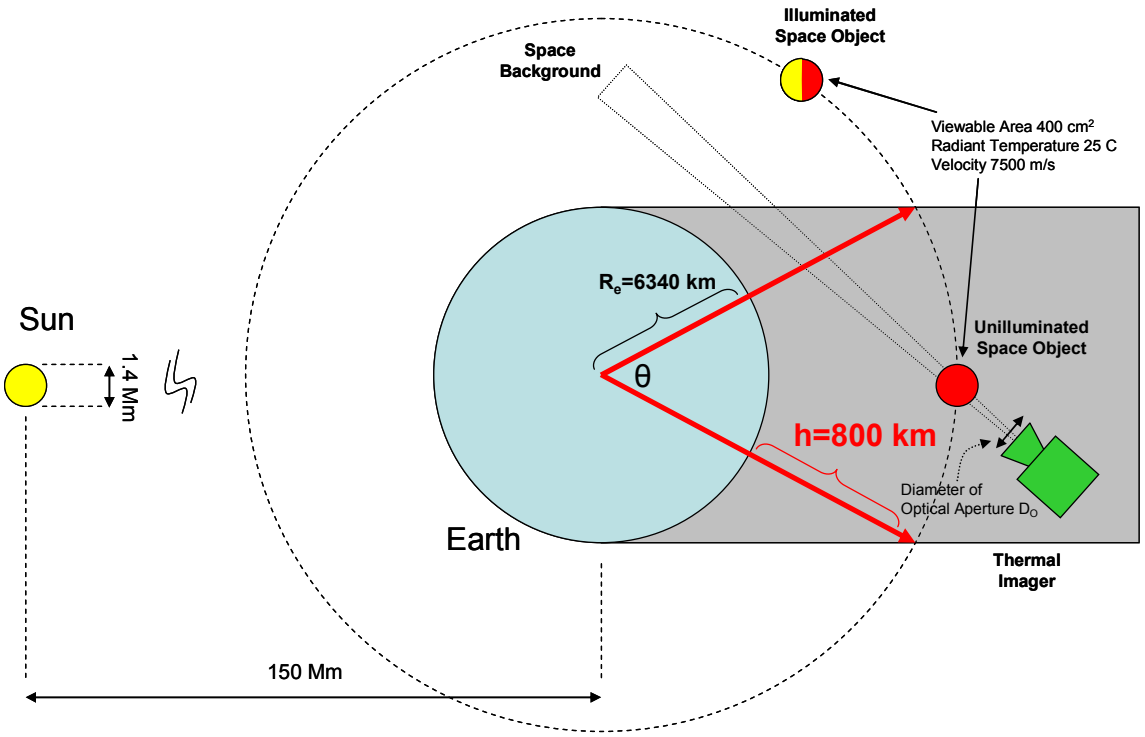

Fig. 1. Shadowing of Low-Altitude Space Objects from Solar Illumination

2. Visible Imager Analysis

In the absence of direct solar illumination, the detection range of a visible system is highly degraded. This can be shown by reviewing the radiometric implication of solar illumination with regard to detection by an imaging system limited by system noise rather than background noise. To quantify these effects, the signal-to-noise ratio (SNR) of

the sensor is expressed as a function of the viewing range R of the imaging system. For this problem, the object is assumed to be a diffuse sphere with reflectivity ρ and apparent area A_T. Furthermore, the solar phase angle is assumed to be 90°. The sensor is characterized by throughput η, noise electrons N_e, and aperture diameter D_O. The SNR of the system is given by Eq. 2.

$$SNR = E_{sol} \frac{2}{3\pi} \frac{\rho}{\pi} A_T \frac{1}{R^2} \frac{\pi}{4} D_O^2 \frac{\eta}{N_e} \tau_{\text{int}} \tag{2}$$

This equation can be simplified and solved for R, as shown in Eq. 3.

$$R = \frac{D_O}{2} \sqrt{\frac{2 A_T E_{sol} \rho \eta \tau_{\text{int}}}{3\pi N_e SNR}} \tag{3}$$

Using Eq. 3, the notional sensor specifications given in Table 1, and assuming that a minimum SNR of 10 is required for detection, the maximum range for detection of the specified object is about 500 km. This is based on the solar flux in the visible band (0.4-0.7 μm) of 1.5E17 ph/s/cm^2. In the absence of sunlight, other sources of illumination such as a full moon would not support a significant detection range. At the surface of the earth, the full moon illuminance is 0.267 lm m^{-2} compared to 1.24E5 lm m^{-2} for the sun, where zenith conditions are assumed for both cases [1]. This indicates that the reduction in illumination when going from direct sunlight to maximum moonlight is a factor of about 5E5. Under these conditions, the detection range is reduced to less than 1 km, neglecting any effects due to the resolution of the target at such a close range. This example demonstrates that the effects of the loss of solar illumination are severe for a visible system to the degree that it is unlikely that the system can perform effectively when the object to be viewed is within earth shadow.

Table 1. Notional Parameters for Visible System Performance Analysis

Parameter	Value
D_T	400 cm^2
η	50%
E_{sol}	1.5E17 ph/s/cm^2
D_O	5 cm
ρ	0.5
N_e	10
τ	15 ms

3. Thermal Imaging Analysis

One solution to the problem of viewing objects that lack solar illumination is to use thermal emissions from the object rather than solar reflections. This idea is manifested in the multitude of multispectral imaging payloads available for airborne surveillance and reconnaissance applications [2][3]. These tactical payloads combine visible imaging and thermal imaging so that the system can operate day or night. For such payloads, adequate spatial resolution is required in order to successfully discriminate targets of interest from ground clutter. Furthermore, target detection requires a sufficient amount of contrast between the target and its background. Typical methods for evaluating performance for these imaging technologies are based on determining the degree of spatial resolution afforded by the available visible or thermal contrast, where the visible contrast includes the effects of illumination under varying conditions [4][5][6]. For thermal imaging systems, the conventional method of performance prediction depends on a figure of merit known as minimum resolvable temperature (MRT). The MRT requires a test observer to determine the required thermal contrast for resolving four-bar targets, if indeed they can be resolved at all. The use of the MRT for predicting performance of tactical thermal imaging systems engaged in surveillance and reconnaissance missions has been prevalent since the introduction of the Night Vision Laboratory Static Performance Model in 1975 [7] and continues to this day.

Unfortunately, the well established models that are used for tactical systems using thermal imagers do not apply to the problem of space surveillance. The primary issue relates to the background. For applications in which the object is both located in space and viewed against the background of space, the background is typically negligible. (Exceptions to this are infrequent and correspond to instances in which there is a conjunction between the space object and a celestial body such as the sun or moon.) For the low background case, the ability to detect the target rests on absolute signal rather than contrast. In addition, the problem of detection is not a matter of spatial resolution but rather signal strength relative to noise sources inherent to the sensor. This is similar to applications of thermal imagers in which targets are viewed against a sky background. For these applications, a signal-based method known as minimum detectable temperature (MDT) is frequently used for performance analysis. The MDT is used when "star detection" is appropriate, which is true for targets viewed against sky backgrounds or space backgrounds [7]. However, even for MDT scenarios, there are discrepancies with the space surveillance application, due to the background influences when viewing airborne targets.

For tactical payloads, it is common to base performance analysis on a standard thermal background, typically at or near 25 C. Furthermore, the thermal sensitivity is normally described in terms of a resolved thermal target using the parameter noise-equivalent temperature difference (NETD). The NETD actually corresponds to a difference in radiance values that generates a signal amplitude equal to the root-mean-square (RMS) noise in the system. For the purpose of determining performance against an unresolved Lambertian source viewed against a background of negligible radiance, the SNR can be computed using Eq. 4, where the target has emissive radiance L_T and the thermal imager has thermal sensitivity *NETD* at 25 C background, optical F-number given by *F*, and square

detectors of width w. The radiometric conversion from temperature difference to radiance difference is accomplished with the differential radiance $\partial L/\partial T$ which is computed for a background temperature of 25 C.

$$SNR = \frac{\tau_O L_T A_T}{NETD \dfrac{\partial L}{\partial T}} \left(\frac{D_O F}{wR} \right)^2 \tag{4}$$

As was done for the analysis of visible imagers, the SNR equation as shown in Eq. 4 can be manipulated to solve for range R_{terr} between the sensor and the terrestrial target. The result is Eq. 5, where the dependency on the radiant intensity $I_T = L_T A_T$ is shown explicitly. This equation shows that performance at a given range depends both on the sensor parameters that are under the influence of the designer and the radiant intensity that must be determined as part of the design process. The final section of this paper addresses considerations for empirical determination of the radiant intensity so that the system performance can be more accurately predicted.

$$R_{terr} = \frac{D_O F}{w} \sqrt{\frac{\tau_O I_T}{SNR \cdot NETD \dfrac{\partial L}{\partial T}}} \tag{5}$$

There are cases of thermal imagers for which Eq. 4 can be used to predict performance of a space-based thermal imager. These correspond to sensors that are limited by system noise even when operating using the minimum temporal bandwidth allowed by the application. For such sensors, reducing the background conditions of the sensor does not improve performance to any significant degree. This is the case for uncooled microbolometers, which use a broad long-wave infrared (LWIR) spectral band of 8 to 12 μm. NETD values of around 50 mK are now attained by devices in mass production [8][9]. Using this value for NETD, and assuming F/1 optics with an aperture diameter of 5 cm, viewing a 25 C target with area of 400 cm^2, a detection range of only 4 km was computed. Since the performance of uncooled microbolometers is limited by system noise and minimum advantage is obtained by virtue of the low background of space, these devices are poor candidates for space surveillance. Fortunately, much better performance can be obtained using cooled devices, so the remainder of this paper is limited to consideration of these thermal imagers, which typically are background-limited.

For high-performance cooled staring sensors, the assumption that system noise is dominant at 25 C background is typically not valid. As a result, the high quantum efficiency and relatively low dark current allow significant sensitivity gains to be obtained when viewing objects under low-radiance background conditions. To account for these sensitivity gains, a modified form of Eq. 5 is needed that is based on the effective dark current radiance and the effective radiance due to optical emissions.

Systems that attain background-limited performance for terrestrial applications should see significant improvement when used with a space background regardless of whether they operate in the medium-wave infrared (MWIR) or

LWIR spectral region. However, given similar values for the detector width, F-number, and NETD, the operating range will depend on the factor $L_T^{0.5}\left(\partial L/\partial T\right)^{-0.5}$. This factor can be used to show that an LWIR imager will have 40% greater range compared to an MWIR imager, given the stated assumptions and center wavelengths of 9 μm and 4 μm, respectively. Consequently, for the cases considered here, LWIR technologies are used.

The condition that is generally maintained for cooled FPA sensors is 50% well fill regardless of background conditions. For the standard 25 C background, photocurrent is induced by the combined contributions from the background scene, the emissions from the imaging optics, and the dark current. For a high-performance cooled LWIR sensor with cut-off wavelength of 9.5 μm, NETD of around 15 mK was reported [10] for a detector size of 30 μm and F/2 optics. Even if sensitivity improvements due to reduced background are not considered, on the basis of Eq. 5, there is an improvement in detection range to 11 km compared to the 4 km range achieved using the less sensitive uncooled sensor. However, given reportedly low levels of dark current for these detectors, significant performance increases are possible given the lower background conditions corresponding to the space-based application.

The space-based advantages are an outcome of the relatively low contribution to background made by the optical emissions and the dark current. The effective radiance emitted by the optics can be estimated using Eq. 6, where τ_O is the optical transmittance and T_O is the temperature of the optics. As a rule of thumb, the effective dark current of the FPA should be matched to the optical emissions using a suitable degree of detector cooling given the optical condition. Based on this, an NETD improvement factor assuming a space background can be computed as given in Eq. 7. This improvement factor is used for predicting the operational range R_{space} for space object viewing as given by Eq. 8.

$$L_O = \frac{1-\tau_O}{\tau_O} L(T_O) \tag{6}$$

$$G_{space} = \frac{2\frac{1-\tau_O}{\tau_O} L(T_O) + L(T_A)}{2\frac{1-\tau_O}{\tau_O} L(T_O)} \tag{7}$$

$$R_{space} = \frac{D_O F}{w} \sqrt{\frac{G_{space}\tau_O I_T}{SNR \cdot NETD \frac{\partial L}{\partial T}}} \tag{8}$$

Making the further assumption that the optical temperature is equal to the standard terrestrial background of 25 C results in a simplified expression given by Eq. 9 for the sensitivity gain that applies when viewing against a space background.

$$G_{space} = \frac{1 - \frac{\tau_O}{2}}{1 - \tau_O} \tag{9}$$

Assuming a nominal optical transmittance of 80%, Eq. 6 results in an estimated sensitivity gain of G=3. This leads to increasing detection range to 20 km for the sample case considered here.

4. Empirical Determination of Radiant Intensity

The foregoing section addressed the determination of the detection range for a thermal imaging system based on design parameters and the radiant intensity of the object to be viewed. The radiant intensity is the product of the apparent area of the object A and the radiance L. The effectiveness of the mission depends greatly on the assurance that the objects of interest can be viewed successfully at suitable ranges. The volume of space within which the thermal imager can view objects, and hence the number of objects available for viewing by the system over the course of its mission, vary as the square of the viewing range even if short-range objects with excessive angular tracking rates are not excluded. However, given the likelihood that the velocity of the thermal imager is high relative to that of the object being viewed, the true set of available targets should exclude those at close range. Assuming that the component of the relative velocity normal to the line of sight between the thermal imager and the space object being viewed is 5000 m/s and the maximum tracking rate is 30 °/sec, there is a minimum viewing range of about 10 km. If the radiant intensity of the object were reduced so that the operational range of the thermal imager was only 15 km instead of 20 km as shown in the preceding example, then the number of viewable objects will be reduced by 75%. It is therefore essential to establish the radiant intensity of the objects to be viewed so that design parameters can be adjusted if necessary in order to assure that there is adequate range performance. This section addresses how the aperture sizing can be done for a ground-based thermal imager that could be used to verify the radiant intensity of the space objects.

Assuming that the space-based thermal imager is designed to view an object with a specified radiant intensity at range R_{terr} using aperture with diameter D_O, aperture diameter D_G of a ground-based thermal imager can be obtained by considering the requirements to operate at a longer range and the impairments driven by the sky background and the atmospheric attenuation. It is assumed that the remaining system parameters are invariant, so that the same F-number, detector width, and optical transmittance still apply.

$$D_G = \frac{D_O R_G}{R_{space}} \sqrt{\frac{1}{\tau_{atmos}} \frac{2\frac{1-\tau_O}{\tau_O} L(T_O) + L_{sky}}{2\frac{1-\tau_O}{\tau_O} L(T_O)}} \tag{10}$$

From [11], the sky radiance in the spectral region near 9 μm is 50% or less of the blackbody radiance of a 25 C blackbody, which is the assumed optical temperature. The value of atmospheric transmittance is assumed to be 50%. Given the combined effects of sky radiance and atmospheric attenuation, the radical term is then computed to be a factor of 2. The dominant effect is due to the far greater ranges at which the ground-based thermal image must operate. The ground-based thermal imager views space objects from a range of 1000 km compared to the range of 20 km for the space-based thermal imager, so the ratio $R_g/R_{space}=50$. Combining the two factors, the aperture of the ground-based thermal imager should be 100 times that of the space-based imager. Since the example was worked assuming the space-based thermal imager used a 5 cm diameter aperture, the aperture of the ground-based system should be 500 cm or 5 m.

5. Large Object Viewing

To further illustrate the use of the analytical modeling approach that has been developed, another example problem is presented. In this example, viewing of a large object is considered. Recently, as part of a study of multispectral methods for estimation of space object temperature and emissivity area product, data for the Hubble Space Telescope was reported [13]. Although the data in this report varied significantly, median values for this object were shown to be about 285 K and 40 m^2. Using these data and the same cooled LWIR example as previously considered for the debris example leads to a predicted maximum range of around 500 km. To obtain thermal imaging data from the ground at a range of 1000 km, use of Eq. 10 shows that the aperture diameter need only be about 4 times larger than the space-based imager, or 20 cm. This assumes that the temperature and emissivity area product are similar when viewed from space or from the ground. If viewing from the ground reduces the apparent area or temperature, a larger aperture might be required.

6. Summary

Maturing thermal imaging technologies enable new options for conducting space surveillance. The primary benefit that is offered is continuous surveillance that operates through periods when solar illumination is not available. To establish baseline design parameters for conceptual systems that employ thermal imagers to view space objects, an analytical modeling approach has been developed. Assuming that the space background implies a negligible contribution to background flux due to the scene, equations for gains in thermal sensitivity are given that account for the background flux contributions from optical emissions and dark current.

The modeling approach is posed so that the sensitivity gains and other sensor parameters are combined with the radiant intensity of the target to predict the operational range of the thermal imager. Ensuring that the imager has sufficient range capability can be critical for successful use of a space-based thermal imager due to the high line-of-sight rate that is likely when viewing close-range targets. As a result, in addition to modeling the performance of a space-based imager, the approach addresses the need for viewing the space object from the ground. In this case, there is atmospheric loss, sky radiance, and greater operating range to be considered. These factors are combined in

a simple fashion to obtain a scaling factor defining the size of the aperture required for a ground-based thermal imager capable of viewing the space objects of interest.

References

1. *Electro-Optics Handbook*, TP-135, Burle Industries, Inc., 1974.

2. Sinclair, R. L. and Tritchew, S., "Stabilized FLIR for Long Range Airborne Surveillance," Proc. SPIE, Vol. 2744, 366-372, 1996.

3. Uhl, B., "RecceLite: Tactical Reconnaissance Pod," Proc. SPIE, Vol. 4492, 92-102, 2001.

4. Johnson, J., "Analysis of Image Forming Systems," in *Image Intensifier Symposium*, U.S. Army Research and Development Laboratories, Ft. Belvoir, VA, 249-273, 1958.

5. Owen, P.R., Dawson, J.A., and Borg, E. J., "Solutions to Modeling of Imaging IR systems for Missile Applications: MICOM Imaging IR System Performance Model-90," Proc. SPIE, Vol. 1488, 122-132, 1991.

6. Doe, J., Boettcher, E., and Miller, B., "Identification of ground targets from airborne platforms," Proc. SPIE, Vol. 7300, 2009.

7. Ratches, J. A., et. al., Night Vision Laboratory Static Performance Model for Thermal Viewing Systems, ECOM 7043, U.S. Army Electronics Command, Ft. Belvoir, VA, 1975.

8. Han, C. J., et. al., "Progress in DRS Production Line for Uncooled Focal Plane Arrays," Proc. SPIE, Vol. 5406, 483-490, 2004.

9. Fraenkel, A., et. al., "BIRD640: SCD's High Sensitivity VGA VO_x µ-Bolometer Detector," Proc. SPIE, Vol. 6737, 2007.

10. Tribolet, P., "High performance infrared detectors at Sofradir," Proc. SPIE, Vol. 4028, 438-456, 2000.

11. Kryskowski, D. and Suits, G., "Natural Sources," in The Infrared & Electro-Optical Systems Handbook, Vol. 1: Sources of Radiation, SPIE, Bellingham, WA, 1993.

12. Thomas, M. and Duncan, D., "Atmospheric Transmission," in The Infrared & Electro-Optical Systems Handbook, Vol. 2: Atmospheric Propagation, SPIE, Bellingham, WA, 1993.

13. Paxson, C., et. al., "Space Object Temperature Determination from Multi-Band Infrared Measurements," 348-357, *The 2007 AMOS Technical Conference Proceedings*, Kihei, HI, 2008.